Winter 1-29-2016

Preparation, Characterization, Electrochemistry, and Infrared Spectroelectrochemistry of Ruthenium Nitrosyl Porphyrins Containing η1-O Bonded Axial Carboxylates

Dennis Awasabisah
University of Oklahoma Norman Campus

Nan Xu
University of Oklahoma Norman Campus

Krishna P. Sharmah-Gautam
Southern Illinois University Edwardsville

Douglas R. Powell
University of Oklahoma Norman Campus

Michael J. Shaw
Southern Illinois University Edwardsville, michsha@siue.edu

See next page for additional authors

Authors
Dennis Awasabisah, Nan Xu, Krishna P. Sharmah-Gautam, Douglas R. Powell, Michael J. Shaw, and George B. Richter-Addo

Cover Page Footnote

The redox behavior of a representative set of Ru porphyrin nitrosyls with η^1-O carboxylate ligands reveal that the first oxidations occur at the porphyrin macrocycles. Appending redox-active ferrocenylcarboxylates to the (por)Ru(NO) centers alters the oxidation behavior such that the first oxidations occur on the ferrocenyl moieities. X-ray crystallographic data were obtained for six of these derivatives that show essentially linear RuNO linkages consistent with their $\{RuNO\}^6$ descriptions.

Preparation, Characterization, Electrochemistry, and Infrared Spectroelectrochemistry of Ruthenium Nitrosyl Porphyrins Containing η^1-*O* Bonded Axial Carboxylates

Dennis Awasabisah,[a] Nan Xu,[a,b] Krishna P. Sharmah Gautam,[c] Douglas R. Powell,[a] Michael J. Shaw,*[c] and George B. Richter-Addo*[a]

Abstract: The synthesis, characterization and redox behavior of eight low-spin nitrosyl carboxylate compounds (por)Ru(NO)(η^1-OC(=O)R) (por = T(*p*-OMe)PP: R = Me (**1**), *i*-Pr (**2**), *t*-Bu (**3**), *p*-$C_6H_4NO_2$ (**4**), Fc (**5**), CF_3 (**8**); por = TTP: R = Fc (**6**)) and (T(*p*-OMe)PP)Ru(NO)(OC_6HF_4) (**7**) are reported. The compounds are moderately stable in air as solids. Their IR (KBr) spectral data show υ_{NO}'s in the 1839-1861 range cm^{-1}. The X-ray crystal structures of compounds **1**, **2**, **5**-**7**, and **8** have been determined, and reveal linear RuNO linkages for these formally $\{RuNO\}^6$ complexes. The redox behavior of the compounds at a Pt working electrode were studied in CH_2Cl_2 with NBu_4PF_6 as supporting electrolyte. The compounds display reversible first oxidations. IR spectroelectrochemistry of compounds **1**-**4**, **7** and **8** revealed porphyrin-centered oxidations, whereas the ferrocenylcarboxylate compounds revealed first oxidations at the ferrocenyl moiety followed by second oxidations at the porphyrin macrocycles. Reductions of these compounds are accompanied by loss of the axial ligands.

Introduction

Ruthenium nitrosyl porphyrins containing *trans* *O*-bonded ligands have been utilized as low-spin structural models of their kinetically unstable but biologically-relevant $\{FeNO\}^6$ (por)Fe(NO)(*O*-ligand) (por = porphyrinato macrocycle) congeners. The ferric (por)Fe(*O*-ligand) fragments are present in the active sites of heme catalase,[1-3] the HasA[4, 5] and IsdB[6] heme-binding proteins, and in some natural mutant hemoglobins such as Hb M Boston [α58(E7)His→Tyr] (i.e., alkoxide ligation) and Hb M Milwaukee [β67(E11)Val→Glu] (i.e., carboxylate ligation). Nitric oxide binds to some of these latter complexes to inhibit their function.[7, 8]

The (por)M(NO) moieties containing the group 8 metals are, indeed, interesting from an electrochemistry standpoint, as all three por/M/NO fragments are electroactive. Despite the biological relevance of the ferric nitrosyl *O*-liganded compounds, it is surprising that only two such (por)Fe(NO)(*O*-ligand) complexes have been reported in the literature;[9, 10] however, these complexes are unstable in solution releasing the weakly-bound NO, making it difficult to characterize the redox behavior of the intact complexes. In contrast, the low-spin $\{RuNO\}^6$ (por)Ru(NO)(O-alkoxide) complexes are relatively stable.[11-14] We have been interested in determining the effects of axial *O*-ligand identity on the redox behavior of such (por)Ru(NO)(*O*-ligand) species. We have prepared a representative set of (por)Ru(NO)(carboxylate) complexes (Figure 1) to determine their redox behavior, and have expanded this study to include ferrocenylcarboxylates which allow for the redox behavior to be probed on the potentially four redox sites por/Ru/NO/Fc fragments in the same compound. Interestingly, ferrocene (Fc) moieties have found applications in biology, examples being as conjugates for proteins/DNA/carbohydrates,[15, 16] antibiotics,[17-19] aspirin,[20] antimalarials,[21-23] and anticancer drugs,[24] and even in cytochrome P450 enzyme studies.[25] A portion of this study (compounds **7** and **8**) has been previously communicated.[26]

[a] Department of Chemistry and Biochemistry, University of Oklahoma, 101 Stephenson Parkway, Norman, OK 73019, USA
E-mail: dawas@ou.edu, grichteraddo@ou.edu
Website: nitroso.ou.edu
[b] Division of Mathematics and Natural Sciences, Penn State Altoona, 3000 Ivyside Park, Altoona, PA 16601, USA
[c] Department of Chemistry, Southern Illinois University Edwardsville, Edwardsville, IL 62025, USA. Email: michsha@siue.edu

Supporting information for this article is given via a link at the end of the document.

Results and Discussion

Syntheses

The target (por)Ru(NO)(*O*-carboxylate) compounds **1**-**6** and **8** (por = T(*p*-OMe)PP, TTP) were prepared in 53-88% isolated yields from reactions of their isoamyl alkoxide (por)Ru(NO)(O-*i*-C_5H_{11})[13, 27] precursors with the corresponding carboxylic acids as shown in Figure 1. The aryloxide compound **7** was prepared similarly using the corresponding phenol.

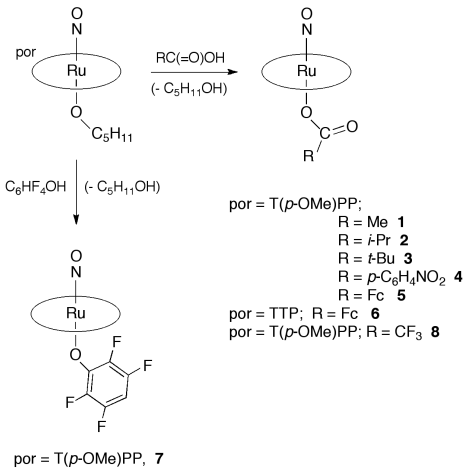

Figure 1. Synthesis of the Ru-carboxylate compounds **1**-**6** and **8**, and the aryloxide compound **7** from the Ru nitrosyl alkoxide precursors.

The reactions typically took ~1 hr to go to completion, as judged by IR spectroscopy. However, the reactions to produce **6** and **8** required longer periods (~12-24 hr) to go to completion, probably due to the weaker acidity of the ferrocenylcarboxylic acid reagent (pK_a of 6.09 (in 50% EtOH),[28] 7.76 (in 80% MeCN),[29] 4.20 (in H_2O)).[30] The products are moderately stable as solids in air at room temperature, showing no signs of decomposition over several weeks as judged by IR and ^{1}H NMR spectroscopy.

Table 1 lists the υ_{NO} and υ_{CO} bands for the (por)Ru(NO)(O-carboxylate) products and the aryloxide compound **7**. The υ_{NO} bands are of these Ru-carboxylates, not unexpectedly, higher than those of the precursor alkoxides (T(*p*-OMe)PP)Ru(NO)(O-*i*-C_5H_{11}) (1801 cm^{-1}) and (TTP)Ru(NO)(O-*i*-C_5H_{11}) (1809 cm^{-1}). The higher υ_{NO} of **8** (at 1861 cm^{-1}, KBr) compared with that of **1** (at 1843 cm^{-1}, KBr) reflects the relative increased electron-withdrawing nature of the *trans* trifluoroacetate with respect to acetate. However, within the compounds **1**, **2** and **3**, the changes in the *trans* axial O_2CCH_3, O_2CCHMe_2, and O_2CCMe_3 ligand did not affect the υ_{NO}s in CH_2Cl_2 in a significant manner.

Table 1. IR nitrosyl and carboxylate stretching frequencies.

Compound	υ_{NO} KBr (CH_2Cl_2)/ cm^{-1}	υ_{CO} KBr (CH_2Cl_2)/ cm^{-1}
1	1843 (1852)	1665 (1647, 1654 sh)
2	1842 (1850)	1666 sh, 1660 (1637, 1642 sh)
3	1839 (1849)	1659, 1653 sh (1640)
4	1849 (1858)	1656 (1651)
5	1840 (1850)	1647 (1634)
6	1839 (1851)	1646 (1634)
7[26]	1844 (1850)	
8[26]	1861 (1866)	1719 (1717)

The υ_{CO} bands of the coordinated carboxylate ligands are also listed in Table 1. In addition to the υ_{CO} band at 1656 cm^{-1} for the *p*-nitrobenzoate ligand of compound **4** (i.e., shifted by 29 cm^{-1} to lower wavenumber from the *p*-nitrobenzoic acid precursor),[31] bands at 1521 and 1302 cm^{-1} were observed and assigned to the υ_s and υ_{as} bands, respectively, of the nitro group. The υ_{CO} band at 1719 cm^{-1} for the ferrocenylcarboxylate compound **8** is downshifted by 64 cm^{-1} from its value in the precursor FcC(=O)OH.

The ^{1}H NMR spectral data for the product complexes are detailed in the Experimental Section. In addition to the signals for the porphyrin macrocycles, new upfield peaks are observed for the *trans* carboxylate ligands. For example, a new peak at -1.47 ppm is observed for the protons of the $CH_3C(=O)O$ ligand in compound **1**, and related upfield peaks at -1.72 ppm and -0.92 ppm are observed for the C*H*$_3$ protons and *H*, respectively, of the $(CH_3)_2CHC(=O)O$ ligand in **2**. The ^{1}H NMR spectrum of the ferrocenylcarboxylate complex **6** shows the peaks due to the four protons of the Cp'-*H* (adjacent to carboxylate) group at 2.70 and 1.70 ppm, and the peak due to the five Cp-*H* protons at 2.38 ppm. Similar upfield shifts of the ferrocenylcarboxylate protons have been observed in the complexes (por)Sn(OC(=O)Fc)$_2$ (por = OEP,[32] TPP[33]).

Molecular structures

The crystal data for the compounds **1**, **2**, **5**, and **6** are summarized in Tables S1-S27 in the Supporting Information, and selected bond lengths and angles for compounds **1**, **2**, and **5**-**8** are listed in Table 2.

Table 2. Selected bond lengths (Å) and angles (deg).

Compound	Ru–N(O)	Ru–O	∠Ru–N–O	∠Ru–O–C
1	1.856(11)	1.909(11)	169.7(14)	131.4(10)
2	1.872(14)	1.807(11)	174.0(12)	127.4(13)
5	1.751(2)	1.996(2)	179.6(3)	131.8(2)
6	1.737(6)	1.968(5)	169.8(7)	135.3(5)
7[26]	1.739(3)	2.000(3)	173.1(3)	127.5(2)
8[26]	1.986(11)	1.773(11)	178.3(9)	134.0(9)

The molecular structures of **1** and **2** are shown in Figures 2 and 3, respectively, whereas the structures of the ferrocenylcarboxylate complexes **5** and **6** are shown in Figure 4.

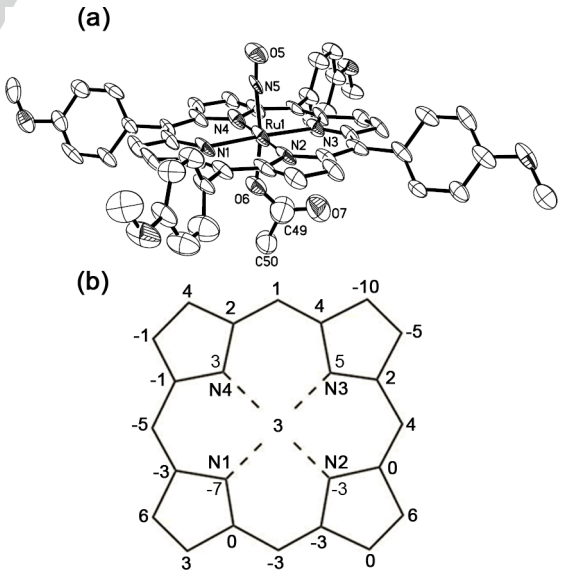

Figure 2. (a): Molecular structure of compound **1**. Hydrogen atoms and disordered molecules have been omitted for clarity. (b): Perpendicular atom displacements (in Å × 100) of the porphyrin core from the porphyrin 24-atom mean plane.

The structures of the tetrafluoroaryloxide compound **7** and trifluoroacetate compound **8** were reported previously.[26] These formally {RuNO}^{6} compounds display essentially linear geometries, with ∠Ru–N–O bond angles in the range 169.6(3)–179.6(3)°. Many of the structural features are not unexpected for these "(por)Ru(NO)X"-type species containing monodentate ligands *trans* to NO. However, three points are worth noting. First, the trifluoroacetate compound **8** has the longest Ru-N(O) bond (Table 2) and the highest υ_{NO} (Table 1) reflecting the weakest overall electron-donating ability of the trifluoroacetate

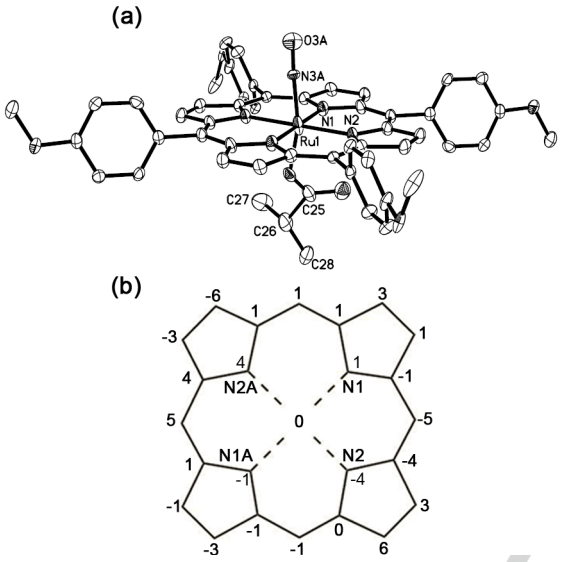

Figure 3. (a) Molecular structure of **2**. Hydrogen atoms and disordered molecules have been omitted for clarity. (b) Perpendicular atom displacements (in Å × 100) of the porphyrin core from the porphyrin 24-atom mean plane.

ligand to the (por)RuNO moiety. Second, the carboxylate ligands bisect the porphyrin N atoms, as determined by the (por)N–Ru–O–C torsion angles for **1** (23.5°), **2** (33.5°), **5** (40.6 °), **6** (25.7°), and **8** (38.0°) with respect to the nearest porphyrin N atom. Third, the Cp'(centroid)-Fe-Cp(centroid) vectors of the ferocenylacetate ligands in **5** and **6** are positioned in essentially parallel orientations with respect to the porphyrin planes in these η^1-carboxylate complexes (Figure 4), although the Fc moiety in **5** is more tilted towards the porphyrin plane than observed in **6** (see Figure S11 in the Supporting Information). Although the ferrocenylcarboxylate ligands are η^1-*O* in our compounds **5** and **6**, η^2-*O*,*O* bonded ferrocenylcarboxylates are present in the compounds Ru(η^2-O_2CFc)(CH=CH_2)(CO)(PPh_3)$_2$[34] and [Ru(η^2-O_2C(L-L)$_2$]PF_6 (L-L = dppm, dppp, dppe).[35]

Electrochemistry

The redox behavior of the carboxylate compounds **1**-**6** and **8**, and the aryoxide compound **7** were investigated by cyclic voltammetry in CH_2Cl_2 at a Pt electrode using NBu_4PF_6 as the supporting electrolyte. The cyclic voltammogram of the aryloxide **7** is shown in Figure 5. The observed first reversible oxidation at $E^{o\prime}$ = +0.59 V versus the Fc/Fc$^+$ couple, to generate the [**7**]$^+$ cation, is 20 mV higher than that required to oxidize

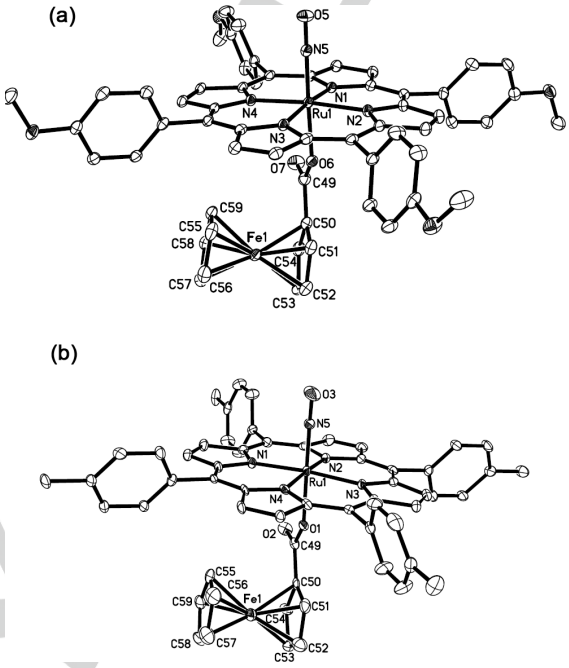

Figure 4. (a) Molecular structure of compound **5**. (b) Molecular structure of compound **6**. Hydrogen atoms have been omitted for clarity.

the related (T(*p*-OMe)PP)Ru(NO)Cl under similar experimental conditions,[36] reflecting the overall better electron-donating property of the aryloxide ligand compared with chloride. The cyclic voltammogram also shows a second reversible oxidation at $E^{o\prime}$ = +1.04 V, and a quasi-reversible reduction at E_{pc} = –1.66 V.

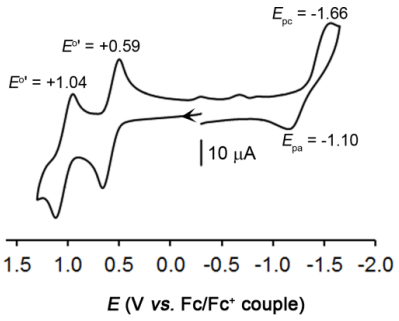

Figure 5. Cyclic voltammogram of **7** showing two oxidations and one reduction. Conditions: 1 mM analyte, 200 mV/s scan rate, 0.1 M NBu_4PF_6 support electrolyte, room temperature.

The cyclic voltammograms of the *alkyl* carboxylate compounds **1**-**3** and **8** are shown in Figure 6. That the first

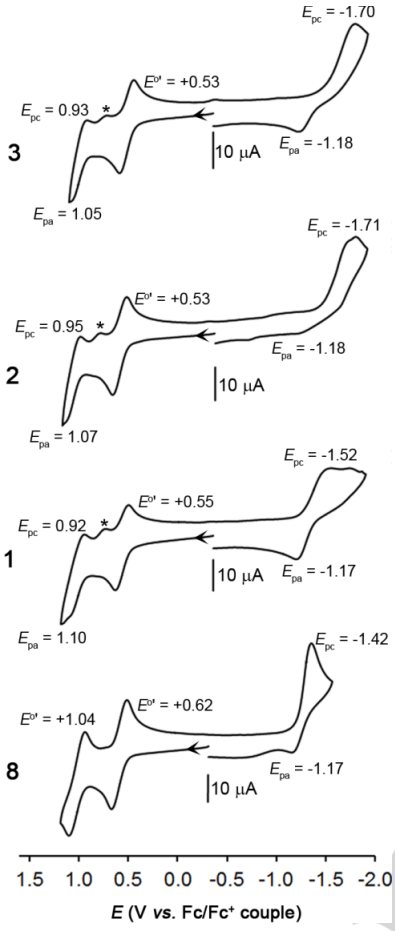

Figure 6. Cyclic voltammogram of compounds **1**-**3** and **8** (1 mM) in CH_2Cl_2 containing 0.1 M NBu_4PF_6 support electrolyte and at a scan rate of 200 mV/s at room temperature. The features labeled * are associated with the return scan after the second oxidations.

reversible oxidation of **3** (trimethylacetate) and **2** (dimethylacetate) are at lower potentials than the acetate complex **1** is not unexpected, an observation rationalized on the basis of the electron-donating abilities of the axial carboxylate ligands; this also parallels the pK_as of the corresponding RC(=O)OH precursors, namely for compounds **8** (R = CF_3; pK_a = 0.5),[37] **1** (R = CH_3; pK_a = 4.75 (in H_2O)),[38] **2** (R = $(CH_3)_2CH$; pK_a = 4.853),[38] and **3** (R = $(CH_3)_3C$; pK_a = 5.031).[37] This is further evidenced by the higher observed potential for the first reversible oxidation of the trifluoroacetate complex **8** (at +0.62 V). The second oxidations for complexes **1**-**3** are close to the solvent limit in our experimental set-up and generally not well-defined, thus were not explored further. The electrochemical reductions, in general, display apparently poor chemical reversibility, and display enhanced cathodic currents (i_{pc}) when compared with the magnitudes of the currents (i_{pa}) for the first oxidations, indicative of follow-up processes such as those involved in *ECE* reactions (see later).

The cyclic voltammogram of the *p*-nitroarylcarboxylate compound **4** is much more defined, and is shown in Figure 7, and bears overall similarity in oxidation behavior with that shown for the aryloxide compound **7** shown earlier in Figure 6, with the first and second reversible oxidations generating $[\mathbf{4}]^+$ and $[\mathbf{4}]^{2+}$, respectively. The cyclic voltammogram also reveals a reduction at E_{pc} = –1.53 V.

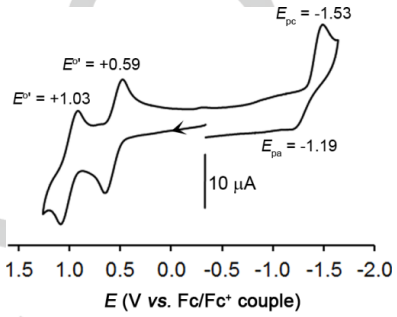

Figure 7. Cyclic voltammogram of **4**. Conditions: 1 mM analyte, 200 mV/s scan rate, 0.1 M NBu_4PF_6 support electrolyte, room temperature.

Examinations of the first reversible oxidations of the alkyl acetate compounds **1**-**3** and **8**, the *p*-nitroaryl acetate compound **4**, and the aryloxide compound **7** reveal that they are diffusion-controlled (with linear plots of i_{pa} vs. $\upsilon^{1/2}$ over the 0.05–1.6 V/s range) and are chemically reversible (with i_{pa}/i_{pc} values of ~1.0).

The preparation of the ferrocenylcarboxylate derivatives **5** and **6** provide systems that contain, in principle, four sites of redox activity; the Ru center, the NO ligand, the porphyrin macrocycle, and the Fc moiety of the *trans* ligand. The cyclic voltammograms of **5** and **6** display some interesting features. Figure 8 shows the redox behavior of compounds **5** and **6**, respectively. The minor return feature between the first and second reversible reductions of compound **5** (top of Figure 8) is only present after the third oxidation is accessed, and is attributed to a minor byproduct from the third oxidation. Based on the magnitude of the redox potentials in Figure 7, we assign the first reversible oxidations to the Fe centers in the ferrocenylcarboxylate ligands; note that the potentials are referenced to the Fc/Fc^+ couple, with the acetyl-Fc/acetyl-Fc^+ couple occurring at +201 mV with respect to Fc/Fc^+ under our conditions (data not shown). Values for the reversible oxidation of ferrocenylacetic acid (+0.05 V in 1,2-dichloroethane),[39] *p*-bromophenylferrocene (+0.09 V in CH_3CN), phenylferrocene (+0.03 V in CH_3CN), octaphenylferrocene (+0.03 V in CH_3CN), and vinylferrocene (+0.02 V in CH_3CN) have been reported.[40] We thus propose that the products from the first reversible oxidations of **5** and **6** are the (por)Ru(NO){$(OC(=O)Fc^+$} cations, where the site of oxidations are the Fe centers (see next section). Related oxidations at the Fe centers in the non-porphyrin ferrocenylcarboxylate complexes Ru(η^2-O_2CFc)(L-L) (L-L = dppm, dppe, dpp)[35] and in (TPP)Sn(OC(=O)Fc)$_2$ are known.[33]

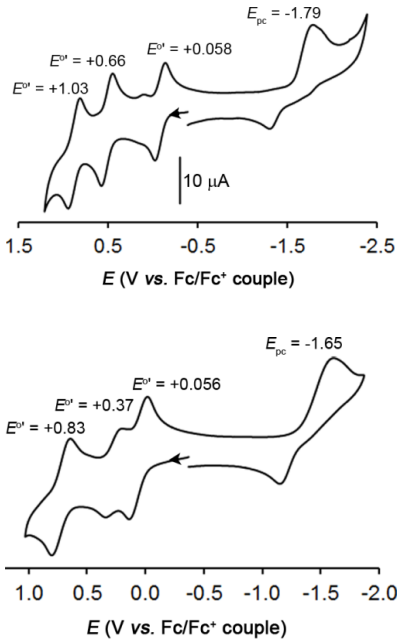

Figure 8. Cyclic voltammograms of **5** (top) and **6** (bottom). [1 mM analyte in CH_2Cl_2, 0.1 M $NBuPF_6$, scan rate of 200 mV s^{-1}].

Infrared spectroelectrochemistry

To help identify the sites of redox behavior and the products that form after oxidations and reductions, IR fiber-optic spectroelectrochemistry experiments were performed using methodology described earlier.[12, 41, 42] In each of these experiments, the Pt working electrode was held at a potential slightly more positive (for oxidations) than the respective peak potential E_{pa}, or slightly more negative (for reductions) than the respective peak potential E_{pc}. The IR spectra of the neutral compounds in support electrolyte were used as backgrounds for the difference spectra.

The data from the difference IR spectra obtained after the first oxidations of the compounds **1**-**8** are summarized in Table 3. In all cases, the observed small magnitudes of $\Delta\upsilon_{NO}$ (~15-21 cm^{-1}) after the first oxidation is indicative of oxidations occurring at locations removed from the RuNO moieties (large $\Delta\upsilon_{NO}$s would suggest greater involvement of the RuNO groups upon oxidation). We note that the related porphyrin oxidations in (T(*p*-OMe)Ru(NO)Me[27] and (OEP)Ru(NO)(OMe)[12] results in larger observed $\Delta\upsilon_{NO}$s of +52 cm^{-1} and +50 cm^{-1}, respectively. The products are thus formulated as the π-radical cations as shown in eq. 1 (por = T(*p*-OMe)PP).

$$(por)Ru(NO)(OR) \rightleftharpoons (por^{\bullet+})Ru(NO)(OR) + e^- \qquad (1)$$

The difference spectra obtained for the oxidations of the aryloxide (non-carboxylate) compound **7**,[26] the trifluoroacetate compound **8**,[26] and the *p*-nitroarylcarboxylate compound **4** are shown in Figure 9 for comparison.

Table 3. IR spectral data (in CH_2Cl_2, cm^{-1}) for the neutral precursors and the generated redox products after the first oxidations.[a]

Compound	Initial		1st oxidation	
	υ_{NO}	υ_{CO}	υ_{NO} ($\Delta\upsilon_{NO}$)	υ_{CO} ($\Delta\upsilon_{CO}$)
1	1852	1647	1873 (+21)	1665 (+18)
2	1850	1637	1871 (+21)	1661 (+24)
3	1849	1637	1870 (+21)	1657 (+20)
4	1859	1654	1879 (+20)	1674 (+21)
5	1852	1634	1867 (+15)	1665 (+31)
6	1850	1634	1865 (+15)	1665 (+31)
7	1850	-	1870 (+20)	-
8	1866	1715	1886 (+20)	1723 (+8)

[a] Experimental conditions: 1 mM analyte, 0.1 M NBu_4PF_6.

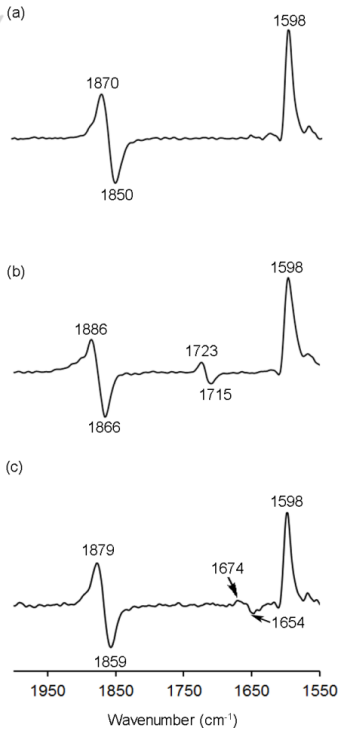

Figure 9. Difference IR spectra obtained during the first oxidations of (a) **7**, (b) **8** and (c) **4** showing the formation of products.

In addition to the observed $\Delta\upsilon_{NO}$s, changes are observed in the 1650-1750 cm^{-1} region, specifically a new band at 1723 cm^{-1} for

8 and 1674 cm^{-1} for **4**, that are not observed in the non-carboxylate compound **7**. These are associated with the υ_{CO}s of the coordinated carboxylates in the π-radical cation products. That the small change in the υ_{CO} region of compound **4** ($\Delta\upsilon_{CO}$ = +21 cm^{-1}) is of similar magnitude to the $\Delta\upsilon_{NO}$ is consistent with the notion that the first oxidation occurs at a site remote from the axial ligand (i.e., eq 1). The new positive features at 1598 cm^{-1} in Figure 9 are associated with an enhancement in intensity of a porphyrin vibration upon oxidations as observed previously for related tetraarylporphyrin systems.[27, 43]

The difference IR spectra obtained after the second oxidations of **4**, **7** and **8** are shown in Figure 10. Here, the

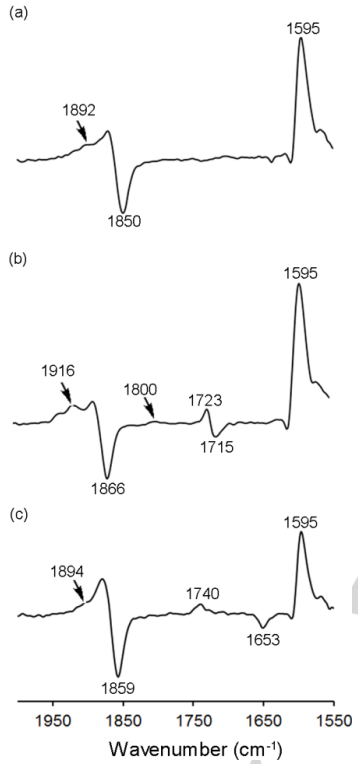

Figure 10. Difference IR spectra obtained during the second oxidations of (a) **7**, (b) **8** and (c) **4** showing the formation of products.

the electrogenerated products are not as well defined, and the new υ_{NO} bands appear as shoulders that are present together with the υ_{NO}s of the first oxidation products, a feature not uncommon for such systems. The small $\Delta\upsilon_{NO}$s between the first and second oxidations also suggest that both oxidations occur on the porphyrin macrocycles. We note that some Ru^{II} porphyrin complexes with π-acids such as CO also display two porphyrin-centered one-electron oxidations.[44]

Electrochemical reduction of the aryloxide compound **7** and the trifluoroacetate compound **8** on our spectroelectrochemical time scale results in the loss of the initial υ_{NO} bands with new bands at 1634 cm^{-1} (for **7**) and 1687 cm^{-1} (for **8**) as shown in Figures 11a and 11b, respectively. Kaim and workers[45] have shown large $\Delta\upsilon_{NO}$ values (~300 cm^{-1}) upon RuNO-centered reduction of some $[(por)Ru(NO)(N\text{-base})]^+$ complexes. However, the bands observed in Figures 11a and 11b are coincident with those of $NaOC_6HF_4$/15-crown-5 and

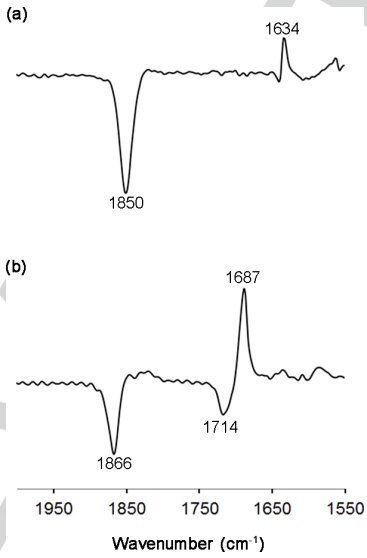

Figure 11. Difference IR spectra obtained during the reductions of (a) **7** and (b) **8** showing the formation of products.

$NaOC(=O)CF_3$/15-crown-5 under our experimental conditions (i.e., in CH_2Cl_2/NBu_4PF_6), indicative of axial ligand dissociation upon the reductions. As noted in the earlier section and from Figure 6, the reductions of the compounds probably involve both electrochemical and chemical steps, and deciphering these will be the subject of future work.

The IR spectroelectrochemical results for the ferrocenylcarboxylate compounds **5** and **6** are shown in Figure 12, and provide further evidence for our assignments of redox activities. The first oxidations of both **5** and **6** similarly result in small $\Delta\upsilon_{NO}$ changes of +15 cm^{-1} (Figure 12a). However, the carbonyl $\Delta\upsilon_{CO}$ changes are +31 cm^{-1} which are *larger* than those seen for the other carboxylate compounds **1**-**4** ($\Delta\upsilon_{CO}$ = +17-24 cm^{-1}) and **8** ($\Delta\upsilon_{CO}$ = +8 cm^{-1}). This observation of larger $\Delta\upsilon_{CO}$ shifts in **5** and **6** are indeed consistent with our assignment of the first oxidation occurring at the Fc centers rather than at the porphyrin macrocycles (eq 2).

$$(por)Ru(NO)(OC(=O)Fc) \rightleftharpoons (por)Ru(NO)(OC(=O)Fc^+) + e^- \quad (2)$$

The spectral results from second oxidation (Figure 12b) reveal new products with υ_{NO} spectral features appearing as a shoulder at 1881 cm^{-1} (for oxidation of **5**) and a new band at 1882 cm^{-1} (for oxidation of **6**). The new peaks in the 1700-1760 cm^{-1} region are tentatively assigned to the υ_{CO}s of the second oxidation products. Notably, enhancements of bands at ~1600 cm^{-1} also indicate that the second oxidation occurs at the porphyrin macrocycles in these complexes (eq. 3).

$$(por)Ru(NO)(OC(=O)Fc) \rightleftharpoons (por^{\bullet+})Ru(NO)(OC(=O)Fc^{+}) + e^{-} \quad (3)$$

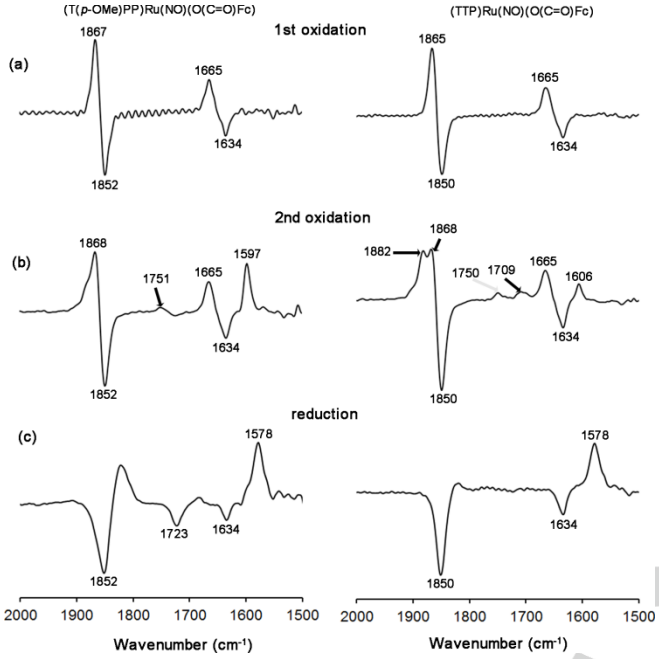

Figure 12. Difference IR spectra of (T(*p*-OMe)PP)Ru(NO)(OC(=O)Fc) (**5**) (left) and (TTP)Ru(NO)(OC(=O)Fc) (**6**) (right) showing the formation of products after (**a**) first oxidation, (**b**) second oxidation, and (**c**) reduction.

The reduction behaviors of **5** and **6** are similarly complex, and generally result in new IR bands at 1578 cm^{-1} (Figure 12c) assigned to the loss of the ferrocenylcarboxylate ligand in solution under the reduction conditions. The broad new peak at ~1810 cm^{-1} for the reduction of **5** signifies perhaps a reduction product at the electrode surface that retains, at least in part,the RuNO fragment prior to NO release.

In any event, the IR spectroelectrochemical data for the ferrocenylcarboxylate compounds **5** and **6** clearly establish that the first oxidation occurs at the axial ligands *trans* to NO in these species.

Experimental Section

General: All reactions were performed under an atmosphere of nitrogen using standard Schlenk glassware and/ or in an Innovative Technology Labmaster 100 Dry Box unless stated otherwise. Solvents for reactions were collected under a nitrogen atmosphere from a solvent purification system (Innovative Technology, Inc. Newburyport, MA, PS-400-5MD) using a glass syringe. The compounds (por)Ru(NO)(O-*i*-C_5H_{11}) (por = H_2T(*p*-OMe)PP = tetra(*p*-methoxyphenyl)porphyrin, H_2TTP = tetra(*p*-tolyl)porphyrin) were prepared as reported in literature for the preparation of the related (TPP)Ru(NO)(O-*i*-C_5H_{11}) compound.[13, 27] Chloroform-*d* ($CDCl_3$, 99.96 atom %D) was purchased from Cambridge Isotope Laboratories, deaerated, and dried under 4 Å molecular sieves. The compounds 2,3,5,6-tetrafluorophenol (C_6HF_4OH, 97%), trifluoroacetic acid ($CF_3C(=O)OH$, 99%), trimethylacetic acid ($(CH_3)_3CC(=O)OH$, 99%), isobutyric acid ($(CH_3)_2CHC(=O)OH$, 99%), *p*-nitrobenzoic acid (*p*-NO_2-$C_6H_4C(=O)OH$, 98%), ferrocene (Fc, 98%), acetylferrocene (AcFc, 95%), ferrocenecarboxylic acid, FcC(=O)OH, 97%), tetrabutylammonium hexafluorophosphate (NBu_4PF_6, ≥99%) and anhydrous methanol (99.8%) were purchased from Sigma-Aldrich and used as received. Acetic acid ($CH_3C(=O)OH$, 99.7%) was purchased from EMD Chemicals and used as received. Dichloromethane for electrochemical experiments was purchased from Sigma-Aldrich and distilled from CaH_2 under N_2 prior to use.

Instrumentation/ Spectroscopy: Infrared spectra were recorded on a Bio-Rad FT-155 and/or a Tensor 27 FTIR spectrometer. ^{1}H NMR spectra were obtained on a Varian 300 MHz spectrometer at 20 °C and the signals referenced to the residual signal of the solvent employed ($CHCl_3$ at 7.24 ppm). ^{19}F NMR spectral signals were referenced to $C_6H_5CF_3$ set to −63.72 ppm. Coupling constants are reported in Hz. ESI mass spectra were obtained on a Micromass Q-TOF mass spectrometer. Elemental analyses were obtained by the staff of Atlantic Microlab, Norcross, GA.

Electrochemistry: Cyclic voltammetric measurements were performed using a BAS CV 50W instrument (Bioanalytical Systems, West Lafayette, IN). In all the electrochemical experiments, a three-electrode cell was utilized and consisted of a 3.0-mm diameter Pt disk working electrode, a Pt wire counter electrode, and a Ag/AgCl reference electrode.[12, 41, 42] Solutions were deaerated before use by passing a stream of N_2 gas through the solution for a minimum of 10 min. A blanket of N_2 was maintained over the solution while performing the experiment; care was taken to minimize evaporative cooling due to N_2 flow in the headspace, as this could cause rolling baselines in the resulting IR difference spectra. The electrochemical experiments were performed in solutions containing 0.1 M NBu_4PF_6 and 1.0 mM of the analyte. Ferrocene, Fc (1.0 mM) was used as internal standard for the electrochemical experiments and potentials were referenced to the Fc/Fc^+ couple at 0.00 V. In cases where the Fc/Fc^+ couple overlapped with the responses of the analyte, the sample was referenced to the $AcFc/AcFc^+$ couple (Ac = acetylferrocene), which was in turn referenced to the Fc/Fc^+ couple. A Bruker Vector 22 and/ or a Tensor 27 FTIR spectrometer equipped with a mid-IR fiber-optic dip probe and liquid nitrogen cooled MCT detector (RemSpec Corporation, Sturbridge, MA, USA) were used for the infrared spectroelectrochemistry. [12, 41, 42] The electrochemical experiments were performed in triplicate to determine reproducibilities. X-ray diffraction data were collected using a diffractometer with a Bruker APEX ccd area detector and graphite-monochromated Mo Kα radiation (λ = 0.71073 Å).

Preparation of (T(*p*-OMe)PP)Ru(NO)(OC(=O)CH_3) (1): To a stirred dichloromethane solution (10 mL) of (T(*p*-OMe)PP)Ru(NO)(O-*i*-C_5H_{11}) (50.3 mg, 0.053 mmol) at room temperature was added excess glacial acetic acid (0.2 mL) and the resulting mixture heated to reflux. During this period the color of the solution changed from red to brown-green. After 1 hour of refluxing the solution was allowed to cool to room temperature and the volume slowly reduced in vacuo to *ca.* 3 mL. Hexane (10 mL) was added and the solution slowly removed in vacuo to *ca.* 5mL to result in the precipitation of a solid. The supernatant was removed with a Pasteur pipette, and the residue washed twice with hexane. The resulting product was then dried in vacuo to give (T(*p*-OMe)PP)Ru(NO)(OC(=O)CH_3) (35 mg, 72% isolated yield). Slow evaporation of a CH_2Cl_2/ cyclohexane (3:1 ratio; 5 mL) solution of the product at room temperature provided suitable crystals for X-ray diffraction studies. IR (CH_2Cl_2, cm^{-1}): υ_{NO} = 1852 s, υ_{CO} = 1647 m, 1654

m (sh). IR (KBr, cm^{-1}): υ_{NO} = 1843 s, υ_{CO} = 1665 m; also 1606 m, 1511 m, 1461 w, 1440 w, 1350 m, 1244 s, 1174 s, 1019 s, 1009 m, 809 m, 798 m, 712 w, 610 w. ^{1}H NMR ($CDCl_3$, 300 MHz): δ 9.00 (s, 8H, *pyrrole*-H of T(*p*-OMe)PP), 8.15 (*app d*, *J* = 8.7 Hz, *J* = 7.8 Hz, 8H, *o*/ *o'*-H of T(*p*-OMe)PP), 7.29 (*app* d, *J* =7.5 Hz, *J* = 7.2 H, 8H, *m/ m'*-H of T(*p*-OMe)PP), 4.10 (s, 12H, OCH_3), −1.47 (s, 3H, CH_3). ESI mass spectrum (TOF): *m/z* 946.3 [M + Na^+] (45%), *m/z* 864.3 [(T(*p*-OMe)PP)Ru(NO)]$^+$ (100%). Anal. Calcd for $C_{50}H_{39}N_5O_7Ru{\cdot}0.5CH_2Cl_2$: C, 62.83; H, 4.18; N, 7.25. Found: C, 62.96; H, 4.09; N, 7.38.

Preparation of (T(*p*-OMe)PP)Ru(NO)(OC(=O)CH(CH_3)$_2$) (2): To a stirred dichloromethane solution (10 mL) of (T(*p*-OMe)PP)Ru(NO)(O-*i*-C_5H_{11}) (50.1 mg, 0.053 mmol) at room temperature was added excess isobutyric acid and the mixture was refluxed for 1 h. During this period the color of the solution changed from red to brown-green. The solution was then allowed to cool, and the volume reduced under vacuum to ~2 mL. Hexane (10 mL) was added and the product mixture was placed in a −20 °C freezer overnight. The resulting precipitate was collected by filtration and dried under vacuum to give 39 mg (77% isolated yield) of the product. Slow evaporation of a CH_2Cl_2/cyclohexane (2:1 ratio; 5 mL) solution of the product at room temperature under nitrogen gave suitable crystals for X-ray diffraction studies. IR (CH_2Cl_2, cm^{-1}): υ_{NO} = 1850, υ_{CO} = 1637 w, 1642 w (sh). IR (KBr, cm^{-1}): υ_{NO} = 1842 s, υ_{CO} = 1666 sh, 1660 m; also 1606 s, 1528 m, 1510 s, 1492 w, 1459 w, 1437 w, 1348 m, 1287 m, 1243 s, 1174 s, 1107 w, 1068 w, 1018 s, 1009 s, 848 w, 807 m, 800 m, 787 w, 715 w, 606 m, 539 m. ^{1}H NMR ($CDCl_3$, 300 MHz): δ 8.99 (s, 8H, *pyrrole*-H of T(*p*-OMe)PP), 8.21 (dd, *J* = 8.6 Hz, *J* = 2.4 Hz, 4H *o*-H of (T(*p*-OMe)PP), 8.08 (dd, *J* = 8.1 Hz, *J* = 2.4 Hz, 4H of *o'*-H of (T(*p*-OMe)PP), 7.28 (*app* d, *J* = 10.2 Hz, *J* = 2.4 Hz, 8H, *m*-H of (T(*p*-OMe)PP), 4.10 (s, 12H, OCH_3), −0.93-(−0.90) (m, *J* = 6.3 Hz, 1H, CH), −1.72 (d, *J* = 6.3 Hz, 6H, CH_3). ESI mass spectrum (TOF): *m/z* 974.3 [M + Na^+] (40%), *m/z* 864.3, [(T(*p*-OMe)PP)Ru(NO)]$^+$ (100%). Anal. Calcd for $C_{52}H_{43}N_5O_7Ru{\cdot}0.2CH_2Cl_2$: C, 64.77; H, 4.52; N, 7.24. Found: C, 64.80; H, 4.71; N, 7.19.

Preparation of (T(*p*-OMe)PP)Ru(NO)(OC(=O)C(CH_3)$_3$) (3): To a stirred dichloromethane solution (10 mL) of (T(*p*-OMe)PP)Ru(NO)(O-*i*-C_5H_{11}) (50.1 mg, 0.053 mmol) at room temperature was added excess trimethylacetic acid and the mixture refluxed for 1 h. During this period the color of the solution changed from red to brown-green. The solution was allowed to cool and the volume reduced under vacuum to ~2 mL. Hexane (10 mL) was added and the solution placed in a −20 ° C freezer overnight. The resulting precipitate was collected by filtration and dried under vacuum to give 38 mg of the product (75% isolated yield). IR (CH_2Cl_2, cm^{-1}): υ_{NO} = 1849 s , υ_{CO} = 1640; IR (KBr, cm^{-1}): υ_{NO} = 1839 s, υ_{CO} = 1659 m, 1653 m; also 1607 m, 1512 m, 1496 w, 1438 w, 1349 m, 1290 m, 1244 s, 1175 s, 1019 s, 1010 m, 849 w, 808 m, 800 m, 788 w, 714 w, 608 w. ^{1}H NMR ($CDCl_3$, 300 MHz): δ 8.98 (s, 8H, *pyrrole*-H of T(*p*-OMe)PP), 8.20 (app d, *J* = 7.2 Hz, 4H *o*-H of (T(*p*-OMe)PP), 8.06 (app d, *J* = 7.5 Hz (*o'*-H of (T(*p*-OMe)PP), 7.30 (*app* d, *J* = 8.7 Hz, 8H, *m*-H of (T(*p*-OMe)PP), 4.09 (s, 12H, OCH_3), −1.66 (s, 9H, CH_3). ESI mass spectrum (TOF): *m/z* 988.4 [M + Na^+] (30%). *m/z* 864.3 [(T(*p*-OMe)PP)Ru(NO)]$^+$ (100%).

Preparation of (T(*p*-OMe)PP)Ru(NO)(OC(=O)C_6H_4-*p*-NO_2) (4): To a dichloromethane (10 mL) solution of (T(*p*-OMe)PP)Ru(NO)(O-*i*-C_5H_{11}) (33.0 mg, 0.035 mmol) was added *p*-nitrobenzoic acid (10 mg, 0.059 mmol). The mixture was stirred overnight during which time the color of the solution changed from red to brown. The solution was reduced to *ca*. 5 mL, and hexane (15 mL) was added. The solution was then placed in a −20 °C freezer overnight. The resulting solid was collected by filtration, washed twice with hexane and dried in vacuo to give (T(*p*-OMe)PP)Ru(NO)(OC(=O)C_6H_4-*p*-NO_2) (29 mg, 81% isolated yield). IR (CH_2Cl_2, cm^{-1}): υ_{NO} = 1858 s, υ_{NO_2} = 1523 s, υ_{CO} = 1651w; IR (KBr, cm^{-1}): υ_{NO} = 1849 s, υ_{NO_2} = 1521 s, 1302 s, υ_{CO} = 1656 m; also 1606 s, 1511 s, 1495 m,1463 w, 1439 w, 1411 m,1349 m, 1288 s, 1245 s, 1175s, 1107 w, 1073 w, 1019 s, 1013 m, 849 w, 811 m, 799 m, 724 w, 714 w, 609 w. ^{1}H NMR ($CDCl_3$, 300 MHz): δ 9.04 (s, 8H, *pyrrole*-H of T(*p*-OMe)PP), 8.20 (*app* d, *J* = 8.1 Hz, 4H, *o*-H of (T(*p*-OMe)PP), 8.01 (*app* d, *J* = 8.7 Hz, 4H, *o'*-H of (T(*p*-OMe)PP), 7.27 (*app* d, *J* = 9.3 Hz, *J* = 7.2 Hz, 8H, *m*-H of (T(*p*-OMe)PP), 7.03 (d, *J* = 8.4 Hz, 2H, *o*-H of (C_6H_4-*p*-NO_2), 4.55 (d, *J* = 8.4 Hz, 2H, *m*- H of (C_6H_4-*p*-NO_2), 4.10 (s, 12H, OCH_3). Anal. Calcd for $C_{55}H_{40}N_6O_9Ru{\cdot}1.7CH_2Cl_2$: C, 57.99; H, 3.72; N, 7.16. Found: C, 58.50; H, 3.71; N, 6.64.

Preparation of (T(*p*-OMe)PP)Ru(NO)(OC(=O)Fc) (5): To a CH_2Cl_2 (10 mL) solution of (T(*p*-OMe)PP)Ru(NO)(O-*i*-C_5H_{11}) (31.0 mg, 0.033 mmol) in a Schlenk tube was added excess ferrocenecarboxylic acid, FcC(=O)OH (30.0 mg, 0.13 mmol). The mixture was refluxed overnight in the dark during which time the solution changed from red to brown-green. The solution was cooled to room temperature, and the solvent removed in vacuo. The resulting residue was washed with anhydrous diethyl ether (5 mL); for this residue, it was necessary to use a spatula to scrape off the solid stuck on the inner walls of the reaction vessel. The supernatant was removed, and the resulting solid washed thoroughly with diethyl ether until the supernatant was no longer colored. The resulting solid was dried in vacuo to give 30 mg (84 %) isolated yield of the product. IR (CH_2Cl_2, cm^{-1}): υ_{NO} = 1850 s, υ_{CO} = 1634 m. IR (KBr, cm^{-1}): υ_{NO} = 1840 s; also υ_{CO} = 1647 m; also 1606 m, 1511 s, 1495 m, 1464 w, 1454 w, 1374 w, 1350 m, 1288 s, 1245 s, 1174 s, 1106 w, 1072 w, 1020 s, 848 w, 811 m, 798 m, 712 w, 608 w. ^{1}H NMR ($CDCl_3$): δ 9.02 (s, 8H, *pyrrole*-H of T(*p*-OMe)PP), 8.16 (*app* d, *J* = 9.3 Hz, *J* = 8.4 Hz, 8H, *o*/ *o'*-H of T(*p*-OMe)PP), 7.28 (*app* d, *J* = 9.3 Hz, 8H, *m*-H of (T(*p*-OMe)PP), 4.12 (br s, 5H, Cp-H), 4.10 (s, 12H, OCH_3), 3.01 (s, 2H, Cp-*H* to adjacent C(=O)), 2.40 (s, 5H, Cp-*H*), 1.71 (s, 2H, Cp-*H* to adjacent C(=O)). Anal. Calcd for $C_{50}H_{45}N_5O_6FeRu{\cdot}0.5CH_2Cl_2$: C, 62.92; H, 4.08; N, 6.17. Found: C, 62.36; H, 4.24; N, 5.98.

Preparation of (TTP)Ru(NO)(OC(=O)Fc) (6): To a dichloromethane (15 mL) solution of (TTP)Ru(NO)(O-*i*-C_5H_{11}) (100 mg, 0.10 mmol) in a Schlenk tube was added excess ferrocenecarboxylic acid, FcC(=O)OH (50.1 mg, 0.21 mmol). The mixture was refluxed for 24 hr during which time the solution changed from red to red-brown. The solution was cooled to room temperature, and the solvent slowly removed in vacuo. The resulting residue was washed with anhydrous diethyl ether (10 mL); for this residue, it was necessary to use a spatula to scrape off the solid stuck on the inner walls of the reaction vessel. The supernatant was removed and the resulting residue washed with twice with anhydrous diethyl ether. The resulting solid was dried in vacuo to give 83 mg (77 % isolated yield) of the product. IR (CH_2Cl_2, cm^{-1}): υ_{NO} = 1851 s, υ_{CO} = 1634 m. IR (KBr, cm^{-1}): υ_{NO} = 1839 s; also υ_{CO} = 1646 m; also 1529 w, 1490 w, 1450 w, 1351 m, 1288 s, 1213 w, 1180 m, 1168 m, 1108 w, 1073 w, 1018 s, 798 s, 716 w, 523 m, 512 m. ^{1}H NMR ($CDCl_3$): δ 9.02 (s, 8H, *pyrrole-H* of TTP), 8.15 (*app* d, *J* = 7.8 Hz, *J* = 2.1 Hz, 8H, *o*/ *o'-H* of TTP), 7.55 (*app* d, *J* = 8.1 Hz, *J* = 1.8 Hz, 8H, *m*-H of (TTP), 3.01 (s, 2H, Cp-*H* adjacent to C(=O)), 2.70 (s, 12H, CH_3), 2.38 (s, 5H, Cp-*H*), 1.70 (s, 2H, Cp-*H* adjacent to C(=O)). Anal. Calcd. for $C_{59}H_{45}N_5O_3FeRu{\cdot}0.3CH_2Cl_2$: C, 67.55; H, 4.36; N, 6.64. Found: C, 67.38; H, 4.66; N, 6.22.

Preparation of (T(*p*-OMe)PP)Ru(NO)(OC_6HF_4) (7):[26] To a stirred dichloromethane (10 mL) solution of (T(*p*-OMe)PP)Ru(NO)(O-*i*-C_5H_{11}) (50 mg, 0.053 mmol) at room temperature was added excess 2,3,5,6-tetrafluorophenol (45.7 mg, 0.284 mmol). The color of the solution changed from red to green on stirring for 30 min. After 4 h of stirring, the volume of the solvent was reduced in vacuo to 2 mL, then 10 mL of hexane was added to aid precipitation of a solid. The supernatant was discarded, and the resulting solid washed with methanol (3 x 15 mL) and

the supernatant discarded each time. The solid was dried overnight in vacuo. Further purification of the solid was accomplished as follows: The solid was dissolved in a minimum amount of CH_2Cl_2 and applied on a neutral alumina (in hexane) column. The column was first eluted with hexane to remove trace unreacted species and byproducts. A green band was then eluted with CH_2Cl_2; this green band was collected and dried in vacuo to afford 43.6 mg (80% isolated yield) of the product. IR (CH_2Cl_2, cm^{-1}): υ_{NO} = 1850 s. IR (KBr, cm^{-1}): υ_{NO} = 1844 s; also 1735 w, 1685 w, 1654 m, 1636 m, 1606 m, 1559 m, 1540 w, 1507 s, 1501 s, 1472 s, 1458 m, 1438 w, 1349 m, 1305 w, 1288 m, 1245 s, 1176 s, 1093 s, 1019 s, 1010 m, 932 m, 848 w, 901 s, 718 m, 607 w. ^{19}F NMR (282 MHz, $CDCl_3$, 20 °C): δ −146.7 (m, 2F) and δ −162.2 (m, 2F). ^{1}H NMR (300 MHz, $CDCl_3$, 20 °C): δ 9.01 (s, 8H, *pyrrole*-H of T(*p*-OMe)PP), 8.17 (d, *J* = 7.2 Hz, 4H, *o*-H of (T(*p*-OMe)PP), 8.08 (d, J_{H-H} = 7.5 Hz, 4H, *o'*-H of (T(*p*-OMe)PP), 7.30 (*app* t (overlapping d's), 8H, *m*/ *m'*-H of (T(*p*-OMe)PP)), 5.29 (m, 1H, *H*-C_6F_4), 4.10 (s, 12H, OCH_3). ESI mass spectrum (TOF): *m/z* = 1052.3 [M + Na^+] (10%), *m/z* = 864.3 [(T(*p*-OMe)PP)Ru(NO)]$^+$ (100%). Anal. Calcd. ($C_{54}H_{37}N_5O_6F_4Ru{\cdot}CH_3OH$): C, 62.26; H, 3.89; N, 6.60 %. Found: C, 62.29; H, 3.61, N 6.74%.

Preparation of (T(*p*-OMe)PP)Ru(NO)(OC(=O)CF_3) (8):[26] A stirred dichloromethane (10 mL) solution of (T(*p*-OMe)PP)Ru(NO)(O-*i*-C_5H_{11}) (50 mg, 0.053 mmol) was treated with excess trifluoroacetic acid (~0.2 mL, ~3 mmol). After stirring for 1 h, the color of the solution changed from red to green. The volume of the solution was reduced to 2 mL in vacuo, and 10 mL hexane was added to aid precipitation of a solid. The supernatant was discarded and the resulting solid was washed with methanol (3 x 15 mL) and the supernatant discarded each time. The crude solid was dried overnight in vacuo. Further purification of the crude solid was accomplished by dissolving it in a minimum amount of CH_2Cl_2 and applying it on a neutral alumina (in hexane) column. The column was first eluted with hexane to remove trace unreacted species and byproducts, and then CH_2Cl_2 was then used to elute a green band which was collected and dried overnight under vacuum to 44.0 mg (85% isolated yield) of the product. IR (CH_2Cl_2, cm^{-1}): υ_{NO} = 1866 s; υ_{CO} = 1717 m. IR (KBr, cm^{-1}): υ_{NO} = 1861 s, υ_{CO} = 1719 m; also 1606 s, 1512 s, 1493 w, 1463 w, 1348 m, 1245 s, 1175 s, 1020 s, 1009 m, 810 m, 800 m, 713 w. ^{19}F NMR (282 MHz, $CDCl_3$, 20 °C): δ −78.1 (s, 3F, CF_3). ^{1}H NMR (300 MHz, $CDCl_3$, 25°C): δ 9.04 (s, 8H, *pyrrole*-H of T(*p*-OMe)PP), 8.20 (d, *J* = 7.8 Hz , 4H, *o*-H of (T(*p*-OMe)PP), 8.10 (d, *J* = 8.1 Hz, 4H, *o'*-H of (T(*p*-OMe)PP), 7.30 (*app* d, *J* = 9.0 Hz, *J* = 8.7 Hz, 8H, *m*/ *m'*-H of (T(*p*-OMe)PP), 4.10 (s, 12H, OCH_3). ESI mass spectrum (TOF): m/z = 1000.1 [M + Na^+] (5%), *m/z* = 864.1 [(T(*p*-OMe)PP)Ru(NO)]$^+$ (100%). Anal. Calcd. ($C_{50}H_{36}N_5O_7F_3Ru{\cdot}CH_2Cl_2$): C, 57.69; H, 3.61; N, 6.60 %. Found: C, 57.62; H, 3.34; N, 6.60%.

Tables of bond lengths and angles for compounds **1**, **2**, **5**, and **6** are contained in the Supporting Information. CCDC 1428260 (compound **1**), CCDC 1428261 (compound **2**), CCDC 1428262 (compound **5**), and CCDC 1428263 (compound **6**) contain the supplementary crystallographic data. These data can be obtained free of charge from The Cambridge Crystallographic Data Center via http://www.ccdc.cam.ac.uk/conts/retrieving.html.

Acknowledgements

This study was supported by the U.S. National Science Foundation (Grants CHE-1213674 to GBRA, and CHE-1213680 to MJS).

Keywords: porphyrin • spectroelectrochemistry • cyclic voltammetry • nitrosyl • carboxylate

[1] P. Nicholls, I. Fita, P. C. Loewen, *Adv. Inorg. Chem.* **2001**, *51*, 51-106.
[2] M. J. Mate, G. Murshudov, J. Bravo, W. Melik-Adamyan, P. C. Loewen, I. Fita, in *Handbook of Metalloproteins, Vol. 1* (Eds.: A. Messerschmidt, R. Huber, K. Wieghardt, T. Poulos), John Wiley and Sons, New York, **2001**, pp. 486-502.
[3] T.-P. Ko, M. K. Safo, F. N. Musayev, M. L. Di Salvo, C. Wang, S.-H. Wu, D. L. Abraham, *Acta Cryst. D* **2000**, *D56*, 241-245.
[4] G. Jepkorir, J. C. Rodriguez, H. A. Rui, W. Im, S. Lovell, K. P. Battaile, A. Y. Alontaga, E. T. Yukl, P. Moenne-Loccoz, M. Rivera, *J. Am. Chem. Soc.* **2010**, *132*, 9857-9872.
[5] P. Arnoux, R. Haser, N. Izadi, A. Lecroisey, M. Delepierre, C. Wandersman, M. Czjzek, *Nat Struct Biol* **1999**, *6*, 516-520.
[6] C. F. M. Gaudin, J. C. Grigg, A. L. Arrieta, M. E. P. Murphy, *Biochemistry* **2011**, *50*, 5443-5452.
[7] N. Purwar, J. M. McGarry, J. Kostera, A. A. Pacheco, M. Schmidt, *Biochemistry* **2011**, *50*, 4491-4503.
[8] G. C. Brown, *Eur. J. Biochem.* **1995**, *232*, 188-191.
[9] N. Xu, L. E. Goodrich, N. Lehnert, D. R. Powell, G. B. Richter-Addo, *Angew. Chem. Int. Ed. Engl.* **2013**, in press. .
[10] N. Xu, D. R. Powell, G. B. Richter-Addo, *Angew. Chem. Int. Ed. Engl.* **2011**, *50*, 9694-9696.
[11] D. S. Bohle, P. A. Goodson, B. D. Smith, *Polyhedron* **1996**, *15*, 3147-3150.
[12] S. M. Carter, J. Lee, C. A. Hixson, D. R. Powell, R. A. Wheeler, M. J. Shaw, G. B. Richter-Addo, *Dalton Trans.* **2006**, 1338-1346.
[13] G.-B. Yi, L. Chen, M. A. Khan, G. B. Richter-Addo, *Inorg. Chem.* **1997**, *36*, 3876-3885.
[14] G.-B. Yi, M. A. Khan, G. B. Richter-Addo, *Chem. Commun.* **1996**, 2045-2046.
[15] D. R. van Staveren, N. Metzler-Nolte, *Chem. Rev.* **2004**, *104*, 5931-5985.
[16] B. Lal, A. Badshah, A. A. Altaf, N. Khan, S. Ullah, *Appl. Organomet. Chem.* **2011**, *25*, 843-855.
[17] D. Scutaru, L. Tataru, I. Mazilu, M. Vata, T. Lixandru, C. Simionescu, *Appl. Organomet. Chem.* **1993**, *7*, 225-231.
[18] E. I. Edwards, R. Epton, G. Marr, *J. Organomet. Chem.* **1976**, *122*, C49-C53.
[19] E. I. Edwards, R. Epton, G. Marr, *J. Organomet. Chem.* **1976**, *107*, 351-357.
[20] M. Sawamura, H. Sasaki, T. Nakata, Y. Ito, *Bull. Chem. Soc. Jpn.* **1993**, *66*, 2725-2729.
[21] C. Biot, G. Glorian, L. A. Maciejewski, J. S. Brocard, O. Domarle, G. Blampain, P. Millet, A. J. Georges, H. Abessolo, D. Dive, J. Lebibi, *J. Med. Chem.* **1997**, *40*, 3715-3718.
[22] F. Dubar, J. Khalife, J. Brocard, D. Dive, C. Biot, *Molecules* **2008**, *13*, 2900-2907.
[23] D. Dive, C. Biot, *Chem. Med. Chem.* **2008**, *3*, 383-391.
[24] S. Top, A. Vessieres, G. Leclercq, J. Quivy, J. Tang, J. Vaissermann, M. Huche, G. Jaouen, *Chem. Eur. J.* **2003**, *9*, 5223-5236.
[25] K. Di Gleria, D. P. Nickerson, H. A. O. Hill, L. L. Wong, V. Fulop, *J. Am. Chem. Soc.* **1998**, *120*, 46-52.
[26] D. Awasabisah, N. Xu, K. P. S. Gautam, D. R. Powell, M. J. Shaw, G. B. Richter-Addo, *Dalton Trans.* **2013**, *42*, 8537-8540.
[27] N. Xu, J. Lilly, D. R. Powell, G. B. Richter-Addo, *Organometallics* **2012**, *31*, 827-834.
[28] A. N. Nesmeyanov, T. V. Baukova, K. I. Grandberg, Y. A. Ustynyuk, S. P. Gubin, E. G. Perevalova, *Izv. Akad. Nauk SSSR; Ser. Khim.* **1969**, 721-723.
[29] G. De Santis, L. Fabbrizzi, M. Licchelli, P. Pallavicini, *Inorg. Chim. Acta* **1994**, *225*, 239-244.

[30] A. A. Pendin, P. K. Leont'evskaya, T. I. L'vova, B. P. Nikol'skii, *Dokl. Adak. Nauk SSSR* **1969**, *189*, 115-118.
[31] M. Yoshida, Y. Katagiri, W. B. Zhu, K. Shishido, *Org. Biomol. Chem.* **2009**, *7*, 4062-4066.
[32] D. Maeda, H. Shimakoshi, M. Abe, M. Fujitsuka, T. Majima, Y. Hisaeda, *Inorg. Chem.* **2010**, *49*, 2872-2880.
[33] H. J. Kim, W. S. Jeon, J. H. Lim, C. S. Hong, H. J. Kim, *Polyhedron* **2007**, *26*, 2517-2522.
[34] L. Matas, I. A. Moldes, J. Soler, J. Ros, A. Alvarez-Larena, J. F. Piniella, *Organometallics* **1998**, *17*, 4551-4555.
[35] I. W. Wyman, T. J. Burchell, K. N. Robertson, T. S. Cameron, M. A. S. Aquino, *Organometallics* **2004**, *23*, 5353-5364.
[36] M. A. El-Attar, N. Xu, D. Awasabisah, D. R. Powell, G. B. Richter-Addo, *Polyhedron* **2012**, *40*, 105-109.
[37] G. W. Gokel, *Dean's Handbook of Organic Chemistry*, 2nd ed., McGraw-Hill, New York, **2004**; pp 8.27, 8.46 and 8.58 (Table 1).
[38] F. G. Bordwell, *Acc. Chem. Res.* **1988**, *21*, 456-463.
[39] M. W. Cooke, T. S. Cameron, K. N. Robertson, J. C. Swarts, M. A. S. Aquino, *Organometallics* **2002**, *21*, 5962-5971.
[40] W. E. Geiger, *J. Organomet. Chem. LIbr.* **1990**, *22*, 142-172.
[41] M. J. Shaw, D. L. Cranford, K. W. Rodgers, J. E. Eilers, B. Noble, A. J. Warhausen, G. B. Richter-Addo, *Inorg Chem* **2010**, *49*, 9590-9598.
[42] M. J. Shaw, R. L. Henson, S. E. Houk, J. W. Westhoff, M. W. Jones, G. B. Richter-Addo, *J. Electroanal. Chem.* **2002**, *534*, 47-53.
[43] D. H. Jones, A. S. Hinman, *J. Chem. Soc., Dalton Trans.* **1992**, 1503-1508.
[44] G. M. Brown, F. R. Hopf, J. A. Ferguson, D. G. Whitten, T. J. Meyer, *J. Am. Chem. Soc.* **1973**, *95*, 5939-5942.
[45] P. Singh, A. K. Das, B. Sarkar, M. Niemeyer, F. Roncaroli, J. A. Olabe, J. Fiedler, S. Zalis, W. Kaim, *Inorg. Chem.* **2008**, *47*, 7106-7113.

Entry for the Table of Contents

FULL PAPER

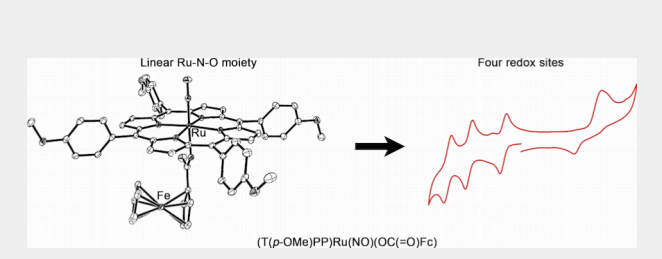

Nitrosyl redox

Dennis Awasabisah, Nan Xu, Krishna P. Sharmah Gautam, Douglas R. Powell, Michael J. Shaw, and George B. Richter-Addo**

Page No. – Page No.

Preparation, Characterization, Electrochemistry, and Infrared Spectroelectrochemistry of Ruthenium Nitrosyl Porphyrins Containing η^1-*O* Bonded Axial Carboxylates

Text for Table of Contents

The redox behavior of a representative set of Ru porphyrin nitrosyls with η^1-*O* carboxylate ligands reveal that the first oxidations occur at the porphyrin macrocycles. Appending redox-active ferrocenylcarboxylates to the (por)Ru(NO) centers alters the oxidation behavior such that the first oxidations occur on the ferrocenyl moieities. X-ray crystallographic data were obtained for six of these derivatives that show essentially linear RuNO linkages consistent with their $\{RuNO\}^6$ descriptions.